Journal of Sound and Vibration (2001) **245**(3), 511–526
doi:10.1006/jsvi.2001.3562, available online at http://www.idealibrary.com on IDEAL®

VIBRATIONAL CONDITIONING OF SURFACE LASER PROCESSING: A FEASIBILITY STUDY

N. K. Anifantis

Machine Design Laboratory, Mechanical and Aeronautics Engineering Department, University of Patras, Patras 26500, *Greece. E-mail: nanif@mech.upatras.gr*

(*Received* 29 *June* 2000, *and in final form* 4 *January* 2001)

In an effort to better understand the laser processes, a vibrational process conditioning technique has been demonstrated utilizing the vibration response changes during laser processing of plate-like workpieces. Taking into account laser processing conditions, the drift of natural frequencies and the disturbance of natural modes of vibration have been computed numerically by means of finite element computational procedures. These simulations reveal a method for conditioning of surface laser processing, based on real-time acquisition and analysis of workpiece vibration response. Material removal by a laser beam produces propagating changes in geometry that decrease the structural stiffness and thus alter continuously the vibration response of the structure being processed, as the machining advances. These flexibilities are properly modelled and evaluated as functions of cutting parameters. A feasibility study has been carried out considering the bending vibration of plate structures with line discontinuities. Numerical results show the sensitivity of the natural frequencies and the disturbances of the natural modes of vibration on the process parameters and thus prove that this non-destructive method may be applied for the conditioning of laser machining processes.

1. INTRODUCTION

Laser machining is a flexible and cost-effective process involving high levels of automation and computational procedures, by which parts with very narrow kerf and excellent surface finishes can be produced. These aspects enable laser machining to become an excellent alternative to traditional machining. This process is based on local heating or precise material removal by applying a highly concentrated light energy obtained by laser irradiation. Laser processing cannot be perceived as simply a laser source, but needs to be considered as an overall system, which includes also driving and controlling systems. These systems need to be specifically tailored to the laser cutting industry and must develop simultaneously. Along with their high degree of automation, laser processes demand advanced monitoring, qualification and conditioning systems, especially in micromachining, biomedical, and difficult-to-access applications, as the influence of all the different operating parameters such as power density, cutting speed, nozzle diameter, beam mode, etc., on the laser cutting process is not definitely clear [1]. The controller parameters can be determined through simulation with the aid of a control model of the laser machining process. Usually, an analytical model of the laser cutting process is developed which would be able to control a computer-integrated laser cutting system for a vast number of different applications. Currently, most laser cutting operating parameters are set by trial and error and apply to one specific application. A highly flexible laser cutting system would increase productivity, efficiency and profit tremendously. This is the incentive for

0022-460X/01/330511 + 16 $35.00/0

developing a proven model of process conditioning. Owing to analytical difficulty in addressing such problems, not much work has been undertaken previously. Various sensing methods which have been developed to monitor laser processes such as ultrasonic, thermographic, or acoustic are sometimes of limited application and accuracy. They realize thermal, optical or acoustic events associated with process evolution [2–5]. Process complexity and description by a large number of parameters reduce the efficiency of these sensing methods some of which present a limited range of application and reliability, giving rise to an ever increasing demand for the development of innovative process conditioning methods, especially for environmentally critical, dangerous and inaccessible regions of process application.

Structural frequency response testing is becoming an integral part of the development and testing of a wide range of industrial and consumer products. It is an essential tool for the definition and solution of many types of structural dynamics problems, such as fatigue, vibration and noise [6, 7]. However, the existence of constraints at any location of a structure causes changes in the natural frequencies of vibration associated with the mode which prevails in the vicinity of this location. Based on this principle, a method for detecting cracks in welded constructions has been developed [8]. The method consists in periodically measuring the natural frequencies, in particular the first three harmonics of the structure or of a part of it. The ratio of the measured frequency to the frequency measured when the structure was first erected gives information on the existence of a defect and furthermore makes it possible to estimate its extent [9].

The possibility of using laser light to impact observable momentum is a well-known technique to excite structures. The method offers a convenient way of studying the elastic properties in thin films under conditions where conventional methods of excitation are difficult [10, 11]. Real-time laser process conditioning from vibration data could prove to be a useful technique. Laser processing offers continuous material and structural changes which reduce the stiffness of the components being processed, as it happens in defective structural members. When a particular structure is processed, some identical parameters appear in the equations that govern the process and in those identifying the structural vibration. This allows for the possibility of using process excited vibration tests to estimate these parameters, and then to use the estimated values to predict the process. Excitation of the workpiece structure by a series of impulsive forces representing the laser beam interaction with the structure surface, may yield information relevant to process conditioning. Given a particular workpiece structure, one can devise simple vibratory experiments, and then the posed problem consists in correlating these characteristics to structural changes due to process advancement. This method of process prediction is based on the information of just the immediately previous stages of the process and may be used in closed-loop control schemes to optimize process conditions. The potential advantage of this non-destructive method is that it is a continuous testing method which may be combined with identification algorithms and finite element procedures.

Figure 1 illustrates a two-dimensional laser machining process in which a plate-like structure is being processed by a laser beam. The beam moves relative to the structure and produces an excavation in the form of a continuous groove. Considering the dimensions of the processed path to be negligible, it takes the shape of a plane curve $\Gamma_g = \Gamma_g(x, y, t)$, defined over the plate surface. The shape of this function clearly depends on the continuous positioning of the laser beam. The formation of this process with associated microcracking and thermal softening of the workpiece material, reduces locally the stiffness of the plate. Apparently, this stiffness reduction depends on the process characteristics, i.e., the extent of the heat-affected zone, its average temperature, and the shape of the excavation. The feasibility of such a purely experimental predictive procedure is investigated in this paper by

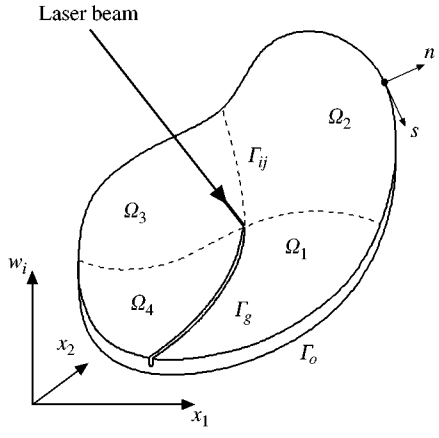

Figure 1. Modelling of a surface laser process.

means of finite element simulations. In these simulations, the distributed restraints arising along the laser processing paths are estimated and their influence on the vibration characteristics of the plates is studied. Then, the correlation between the vibration response characteristics and the laser cutting parameters reveals the limits and the applicability of this non-destructive method.

2. LOSS OF STIFFNESS ALONG A PROCESSED PATH

The presence of an excavation with the shape of a groove or a cut in a sheet-like structure introduces structural modifications associated with a local loss of stiffness. The posed problem is to equivalently substitute this local change in geometry by elastic elements and to correlate the properties of these elements with the aspects of the laser process. The physical behavior of these elements depends on the local behavior of the structure, and simulates the loss of stiffness produced by the laser process.

Figure 2(a) illustrates an idealized cross-section of a machined excavation in a sheet of thickness h. This excavation has depth d and average width $2r$. Considering bending deformations, dominant discontinuities concern mostly transverse displacements and normal slopes along the excavation. Figures 2(b) and (c), illustrate these fundamental modes of deformation which characterize stiffness reduction. The loss of stiffness may then be considered as consisting of two distributed springs along the excavation, one resisting transverse displacements and the other rotations. These elastic elements which are defined per unit length of the excavation, are functions of both the geometry and temperature, and are denoted by the symbols $k_t = k_t(x, y)$ and $k_r = k_r(x, y)$, respectively, where the co-ordinates (x, y) define the position on the excavation path Γ_g. The behavior of the structure along the path of the process may be modelled by a stiffness matrix which involves all possible degrees of freedom existing in this area. However, off-diagonal terms of this matrix are expected to have negligible contribution to the dynamic behavior of the structure, and thus are not considered in this work.

Local flexibilities of structure expressed by line transverse and rotational stiffness elements k_t and k_r, respectively, have been evaluated by the finite element method [12]. Finite element analysis for this model assumes linear elastic material properties and farfield loading conditions corresponding to bending or shearing. Plasticity effects are ignored and

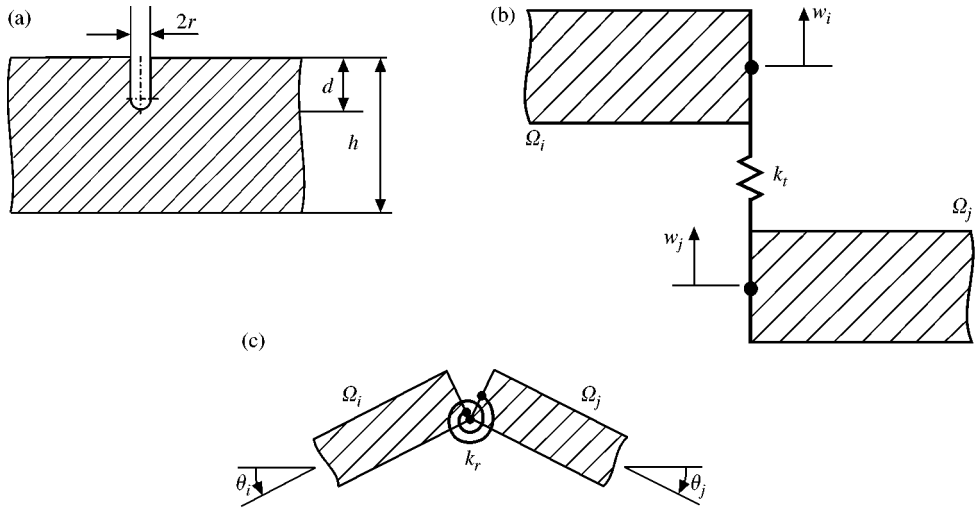

Figure 2. Modelling of a longitudinal excavation produced by a laser beam. (a) Geometry of the cut; (b) transverse stiffness; and (c) rotational stiffness.

the average temperature of the heat-affected zone is considered as degrading equivalently the structural stiffness.

For an idealized groove cross-section like that shown in Figure 2(a), a finite element procedure has been developed for the evaluation of these equivalent springs. A series of solutions were conducted to account for the parameters which identify the process characteristics. From the nodal results of these finite element analyses, the local stiffness constants were found. The numerical results are depicted in Figure 3 for various values of the involved parameters. Line stiffness reduction parameters are defined per unit length and are normalized as follows:

$$K_t = \frac{k_t}{D}\ell^3, \qquad K_r = \frac{k_r}{D}\ell, \tag{1}$$

where ℓ is a reference length, $D = Eh^3/12(1-\nu^2)$ is the flexural rigidity of the plate, E, ν being the Young's modulus and the Poisson ratio respectively.

In Figure 3 these parameters are drawn as functions of the excavation depth, d/h, and for various average temperatures of the heat-affected zone. Numerical results refer to steel sheets with an excavation of width $r/h = 0{\cdot}01$. A detailed numerical investigation has proved that the local stiffness reduction is very sensitive to the process depth and less sensitive to the excavation width and temperature rise. However, the exact shape of the excavation cross-section has little effect on the stiffness reduction, reducing significantly the number of parameters involved in the problem definition. When the groove is enhanced to a through cut, full loss of stiffness occurs, which produces severe structural changes.

Figure 3 correlates the laser machining characteristics defined by the depth of the excavation and the average temperature rise to the structural changes defined by the transverse and rotational stiffness reduction parameters. Thus, it may be adopted as a process identification tool. Furthermore, if one establishes the relation between the stiffness reduction parameters and the vibration response of the same structure, conclusions may be drawn regarding the process condition, because the only unresolved parameters are the shape and the length of the cut.

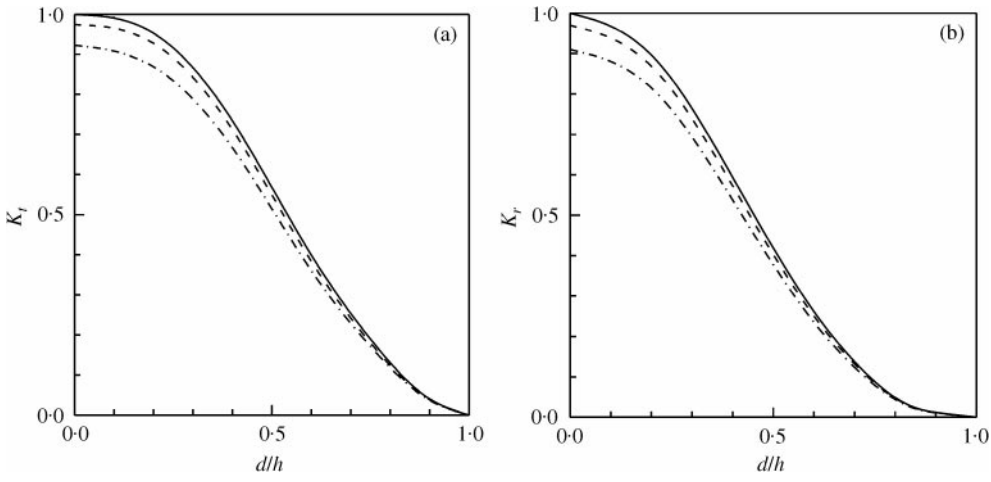

Figure 3. Local stiffness coefficients with process characteristics for $r/h = 0{\cdot}01$. (a) Transverse stiffness; and (b) rotational stiffness: ——, $T = 0°C$; ------, $T = 500°C$; —·—·—·, $T = 1000°C$.

3. ANALYTICAL CONSIDERATIONS

Without loss of generality, the simplest model which can be conceived to illustrate the application of the proposed vibrational laser conditioning technique embodies vibration of uniform plates. Apart from its mathematical simplicity, this model will provide information which exists, but is obscured in more complex structures. For reasons of completeness and to illustrate the analytical difficulties of this modelling, a brief mathematical description is given in the following. Although this mathematical modelling involves the eigenvalue problem of flat plates which contain distributed restraints along laser processed paths and thus presumes quasi-static conditions, the dynamic response and the instantaneous beam velocity can also be incorporated, but this is beyond the scope of the present work. Consequently, in order to investigate the influence of laser processing characteristics on the frequency response of plates, non-propagating cuts are considered and thermal softening is considered along the processed path as discussed earlier.

Consider a thin, isotropic plate which lies in the x–y plane and is of constant thickness h. It is recessed by surface or through cuts with the shape of a line, as those produced by laser marking, scribing, excavation or cutting processes. Depending on the type of process, a laser beam machines a continuous or discontinuous groove which may be considered as a line restraint with zero cross-sectional dimensions and appropriate stiffness characteristics as discussed in the previous section. The solution procedure for the problem of the vibration of plates restrained in such a way, is based on the Mindlin plate theory and the substructuring method, which can be regarded as an alternative form of the finite strip method [13–16]. This substructuring technique via artificial springs has been applied also by Avalos *et al.* [17], and Lee and Ng [18, 19] to predict the dynamic response of plates and skeletal structures with discontinuities respectively. Accounting for the shape of the processed path and its virtual extension, the plate is idealized by substructures. A plate with a narrow groove, starting from the perimeter of the plate is shown in Figure 1.

Let the plate under consideration be cut along the line of excavation, and the effects of the grooved and ungrooved segments be represented by the application of appropriate conditions. If each substructure i, is defined within the subdomain Ω_i, then, the domain of

the problem is

$$\Omega = \sum_{i=1}^{m} \Omega_i, \tag{2}$$

where m is the total number of substructures.

According to small deflection plate theory, the differential equation of free vibration of each substructure is [20]

$$-D\nabla^4 w_i(x, y, t) = \rho h \ddot{w}_i, \quad (x, y) \in \Omega_i,\ i = 1, 2, \ldots, m, \tag{3}$$

where ∇^4 is the biharmonic operator, w_i is the transverse displacement of the ith substructure and ρ the density. It is to be noted that w_i is a function of x, y and time t, and dots represent derivatives with respect to t. The relations between the forces and deformations, in terms of normal and tangential coordinates (n, s) as shown in Figure 1, are

$$M_{in} = -D\nabla^2 w_i + (1-\nu)D\left(\frac{1}{R}\frac{\partial w_i}{\partial n} + \frac{\partial^2 w_i}{\partial s^2}\right), \tag{4}$$

$$M_{ins} = (1-\nu)D\left(\frac{\partial^2 w_i}{\partial n \partial s} - \frac{1}{R}\frac{\partial w_i}{\partial s}\right), \tag{5}$$

$$Q_{in} = -D\frac{\partial}{\partial n}\nabla^2 w_i, \tag{6}$$

where M_{in}, M_{ins} are the normal and tangential bending moment components, Q_{in} the shearing force, and the Laplacian has the form

$$\nabla^2 = \frac{\partial^2}{\partial n^2} + \frac{1}{R}\frac{\partial}{\partial n} + \frac{\partial^2}{\partial s^2}. \tag{7}$$

In the above equations, R denotes the radius of curvature of the boundary curve.

On the outer surface Γ_o of the plate, standard boundary conditions exist depending on the nature of supports. Along the interfaces Γ_{ij} defined between adjacent subdomains Ω_i and Ω_j, standard continuity and compatibility conditions hold, except on the interfaces Γ_g, where the laser excavations exist. Along the latter, deformation and slope discontinuities are established, which in view of equations (4)–(6) can be written as

$$w_i - w_j = Q_{in}/k_t, \qquad \frac{\partial w_i}{\partial n} - \frac{\partial w_j}{\partial n} = M_{in}/k_r \tag{8, 9}$$

respectively. In equations (8) and (9), subscript i means evaluation of associated functions on the boundary surface of the subdomain Ω_i. The discontinuities on transverse displacement and rotation are controlled by the local stiffness coefficients k_t and k_r, respectively, which depend on the local process characteristics, expressed by the machining geometry and the average temperature of the heat-affected zone.

Assuming $w_i(x, y, t) = W_i(x, y)F(t)$ where the function W_i depends on the spatial co-ordinates only, $F(t)$ is a time-dependent harmonic function, and separating the variables equation (3) yields

$$(1 - \lambda^4)\nabla^4 W_i = 0, \quad (x, y) \in \Omega_i,\ i = 1, 2, \ldots, m \tag{10}$$

The parameter $\lambda^4 = \omega^2 \rho h/D$ represents the eigenvalue of the problem and ω is the circular frequency.

The general solution of equations (10) depends on the particular co-ordinate system which more effectively describes the plate and its substructures Ω_i. Furthermore, the eigenvalues of the structure depend on the shape and geometry of the interfacial curve Γ_g and the magnitude of the local flexibilities. Application of equations (8) and (9) and standard continuity, compatibility and boundary conditions yields the characteristic equation of the problem. When the processing lines are straight, the treatment of the problem is mostly trivial. The presence of irregular interfaces resulting from complicated processing demands more advanced techniques. This equivalently means that it is a very difficult task to prepare analytical solutions for the posed eigenvalue problem in a global reference system. For the purposes of the present work, numerical formulations will be utilized in the following, based on the finite element approach, which is the simplest way to exploit this problem. The solution of the eigenvalue problem yields the natural frequencies of the structure and the natural modes of vibration as functions of the stiffness reduction parameters k_t and k_r. The sensitivity of the vibration response to those parameters is expected to determine the feasible domain of the laser machining conditioning problem.

4. NUMERICAL PREDICTIONS AND DISCUSSION

A numerical investigation into cutting conditioning in laser processing of two-dimensional workpieces is presented in this section utilizing finite element procedures. Numerical simulations regarding eigenvalue analysis of rectangular plates with dimensions $a \times b$, subjected to a single line restraint are carried out. The restraint, which has length b_0 and is parallel to the side b at a distance a_0, simulates the effect of an excavation machined by a laser beam (Figure 4). In order to investigate the sensitivity of the response to the supporting method, two different cases have been analyzed, regarding a simply supported and a free edge structure respectively. Parametric studies have been conducted by varying the dimensions of the plate, the length and the stiffness of the discontinuity. For the purposes of the present study and without loss of generality, steel plates were considered with $b = 1$ m, $h = 0{\cdot}01$ m, and the side α as an independent global variable. The material properties of these structures were assumed to be $E = 210$ GPa, $\nu = 0{\cdot}3$ and $\rho = 8000$ kg/m^3. Each plate contains a straight surface excavation of width $r = 50$ μm in the form shown in Figure 2(a), which represents a laser processing path. With reference to the tip of the processing path, four rectangular subdomains can be defined. Each subdomain may be further subdivided into a number of rectangular elements. The line restraint introduced by the laser beam excavation is considered in the model through spring elements distributed along this line. These springs have appropriate stiffness characteristics as discussed earlier, and join adjacent node pairs along the processing path. Their stiffness characteristics depend on the laser process characteristics and may be determined by Figure 3. Numerical results cannot be directly interpreted in terms of the excavation depth because the response depends also on other factors. These involve the position and shape of excavation, operating temperatures, plate dimensions and stiffness, some of which are included in the local stiffness coefficients. These coefficients vary from zero to very high values when through or part through cuts are present respectively. To study the dynamic response qualitatively, a steel plate containing an excavation with constant depth and zero temperature of the heat-affected zone was examined. Then, for a given depth of excavation, the local stiffness coefficients get definite values. The definition of these coefficients per unit

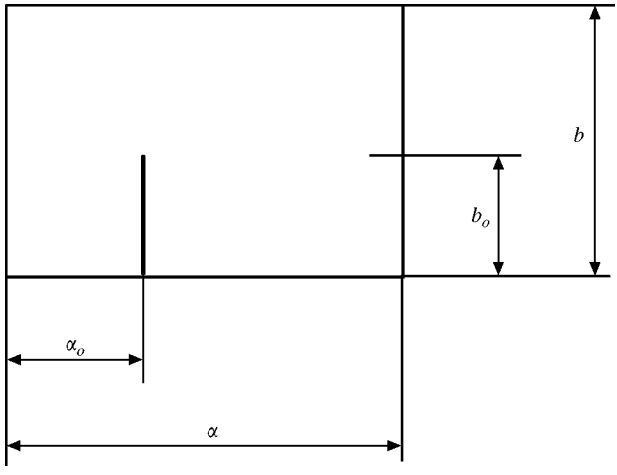

Figure 4. Geometry of a rectangular plate containing a straight excavation.

length of excavation enables the determination of appropriate spring constants depending on plate dimensions and stiffness, as equation (1) indicates. These springs equivalently represent the same loss of stiffness as that defined by coefficients k_t and k_r respectively. When variations in excavation depth or temperature occur, then appropriate averaged values of local flexibility coefficients may be determined by means of Figure 3. This equivalently means that the springs along the excavation path have varying stiffness according to the variations of local flexibility coefficients. In the following computations, for reasons of simplicity $k_t = k_r = k$ was taken, where the parameter k equivalently stands for stiffness constants introduced between the node pairs in which the restraint occurs. Then, according to equations (1), the frequency shift is illustrated as a function of the local flexibility coefficient $C = D/k$, where the reference length is $\ell = b = 1$ m. This coefficient represents equivalently the compliance occurring across the subdomains which are adjacent to the excavation. Small values define shallow excavations, though large values define through cuts respectively.

The accuracy and convergence characteristics of the finite element approach were studied for a free plate with $\alpha = b = 1$ m, without any restraints, the analytical vibration response of which is available elsewhere [20]. The natural frequencies ω_{mn0} of this perfect structure are given then by the equation

$$\omega_{mn0} = \pi^2 \left[\left(\frac{m}{\alpha} \right)^2 + \left(\frac{n}{b} \right)^2 \right] \sqrt{\frac{D}{\rho h}}, \quad m, n = 1, 2, \ldots \ . \tag{11}$$

Vibrational mode shapes are denoted by indices (m, n), where m, n are the numbers of half-waves in the x and y directions respectively. Several finite element models were examined to predict numerically the results of equation (11). In these models, the processed path was approximated by springs of large stiffness (10^{10}) to simulate continuous plates. When each substructure contains a mesh of (4×4) element subdivisions, the numerical solution converges to that expressed by equation (11). The maximum difference is observed on the higher harmonics and is lower than 2·0%.

The accuracy of the numerical procedure was checked also for the case where a simply supported rectangular plate has a through straight cut like a crack. In this case, the stiffness of the springs along the restraint path was taken to be zero. Table 1 shows a comparison

TABLE 1

Analytical and numerical predictions of eigenvalues of simply supported rectangular plates with a straight cut

Mode		Analytical [18]	Numerical	% Difference
Symmetric	11	0·896	0·903	0·7
	21	0·961	0·956	− 0·5
	31	0·981	0·993	1·2
Antisymmetric	12	0·637	0·643	0·6
	22	0·916	0·914	− 0·2
	32	0·889	0·906	1·7

between analytical and numerical predictions of eigenvalues for a plate with $\alpha/b = 0{\cdot}25$, $\alpha/\alpha_0 = 0{\cdot}5$ and $b/b_0 = 0{\cdot}5$. It must be noted here that the analytical predictions regard rectangular plates with through cracks [21]. The predicted numerically natural frequencies were normalized with respect to the corresponding frequencies of the unprocessed perfect structure, i.e.,

$$\lambda_{mn} = \frac{\omega_{mnr}}{\omega_{mn0}}, \quad m, n = 1, 2, \dots , \tag{12}$$

where ω_{mnr} are the natural frequencies of the restrained plate. Numerical results are very close to those analytically predicted with maximum difference lower than 2·0%. Accounting for this information, all subsequent results refer to a finite element model which involves 256 plate elements, 8 spring elements and 333 nodes.

4.1. SIMPLY SUPPORTED PLATE

The eigenvalue problem of a freely vibrating simply supported plate which contains a line excavation was considered initially. This type of restraint may be located at two distinct positions, i.e., at $\alpha/\alpha_0 = 0{\cdot}5$ and $\alpha/\alpha_0 = 0{\cdot}25$. With reference to some selected lower modes of vibration, Figure 5 illustrates the normalized frequency drop λ_{mn} of the plate with the equivalent stiffness representing the contribution of the excavation. The mode of vibration 11 exhibits a very small sensitivity to the presence of the cut showing maximum changes of order 2%. Higher modes ($m \geqslant 1, n \geqslant 1$) show higher sensitivity to the presence of the cut. The aspect ratio of the plate dimensions affects significantly the changes in natural frequencies, as the comparison between Figure 5(a) and (b) shows. The position of the excavation affects also the response as shown by dashed lines in Figure 5. Frequency shifts observed in this figure may be explained more clearly with reference to Figure 6. This latter figure illustrates some lower order natural modes of vibration of a square plate with a restraint having $\alpha/\alpha_0 = 0{\cdot}5$ and $b/b_0 = 0{\cdot}5$. This figure depicts also steep discontinuities in the regions along the line of the excavation. As shown, supporting conditions affect significantly the frequency shift producing a more or less stiff structure. Figure 7 illustrates the effect of the cut length on the frequency drop, for some value of restraint stiffness. The influence of the plate dimensions on the frequency response is apparent. Small length cuts have negligible influence on frequency shift, and large cuts reduce significantly the frequency up to 50% depending on the vibration mode.

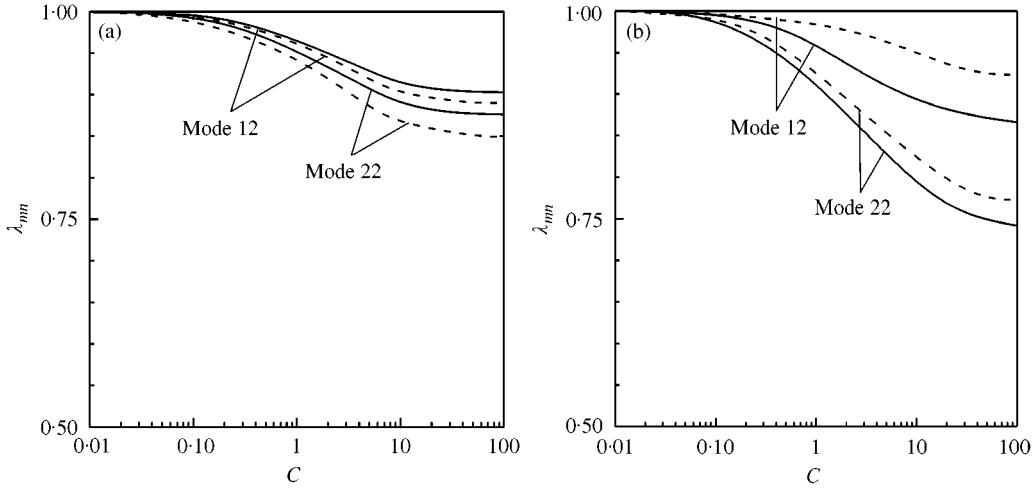

Figure 5. Drift in natural frequencies of simply supported plates with excavation; (a) square, $\alpha/b = 1{\cdot}0$ and (b) rectangular plates, $\alpha/b = 2{\cdot}0$: ——, $\alpha_0/\alpha = 0{\cdot}25$; ------, $\alpha_0/\alpha = 0{\cdot}50$.

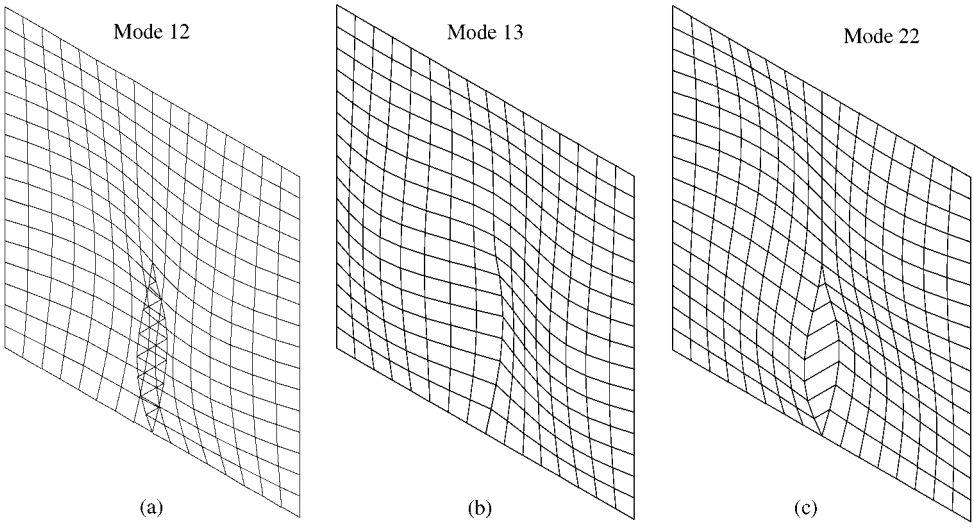

Figure 6. Natural modes of vibration of a square simply supported plate containing a straight excavation.

4.2. FREE PLATE

A freely vibrating plate which contains a line excavation was considered next. Four spring elements attached to the corners of the plate were utilized to simulate free boundary conditions. The stiffness characteristics of these elements were evaluated through the convergence procedure to be of the order 10^2. Figure 8 illustrates the normalized frequency λ_{mn} for some selected lower modes of vibration with the stiffness of the restraint. This structure seems to be more sensitive to the changes in the depth of the cut than the corresponding simply supported one. Lower frequencies are not shown, i.e., the 11 and 12, are invariant to the cut depth. Figure 9 illustrates some natural modes of vibration for the same plate, from which it is apparent that the mode 12 is insensitive to the existence of the

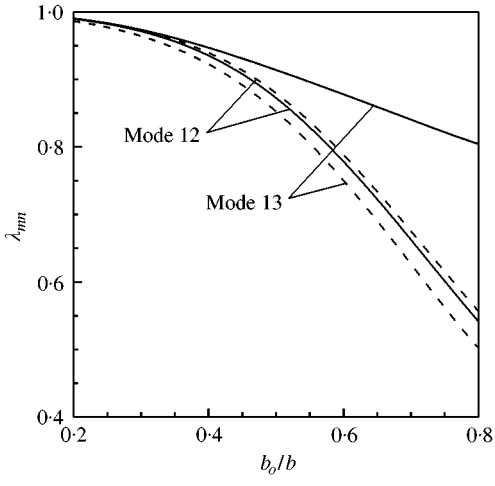

Figure 7. Influence of excavation length on natural frequencies of simply supported plates, when $C = 2{\cdot}0$ and $\alpha_0/\alpha = 0{\cdot}50$: ——, $\alpha/b = 1{\cdot}0$; ------, $\alpha/b = 20$.

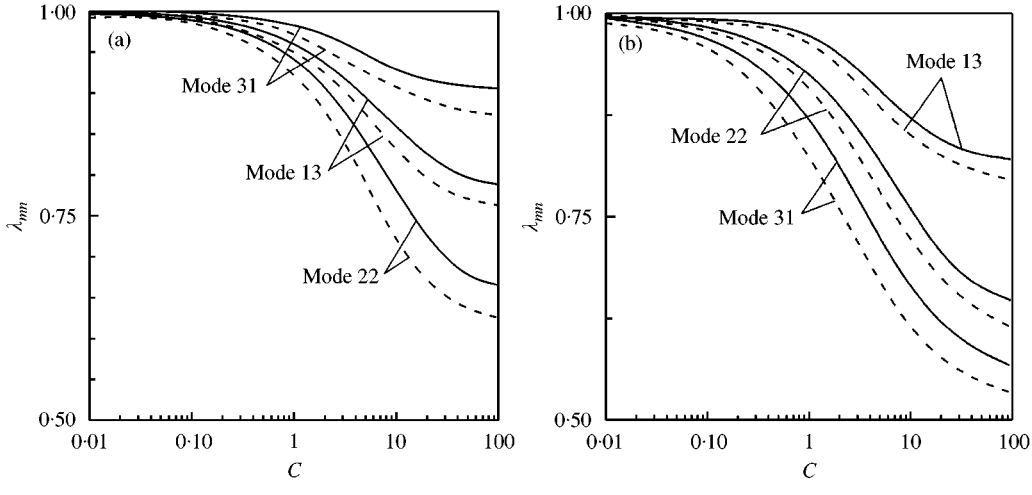

Figure 8. Drift in natural frequencies of free plates with excavation; (a) square, $\alpha/b = 1{\cdot}0$ and (b) rectangular plates, $\alpha/b = 2{\cdot}0$: ——, $\alpha_0/\alpha = 0{\cdot}25$; -------, $\alpha_0/\alpha = 0{\cdot}50$.

cut. The vibration amplitudes and the magnitudes of the discontinuities are in this case lower than those observed in simply supported plates. In the case of free plates, higher frequency shifts occur than those in simply supported plates as Figure 10 depicts. As shown in this figure, free plates are more sensitive to shallow cuts.

4.3. CURVED EXCAVATION

The influence of curved excavations on the dynamic response was examined in a single case concerning a free square plate. The plate has properties and geometry as referred to above and contains a curved excavation of the form of a circular arc with its center located at one corner of the plate, starting point the middle of a corresponding side and radius one

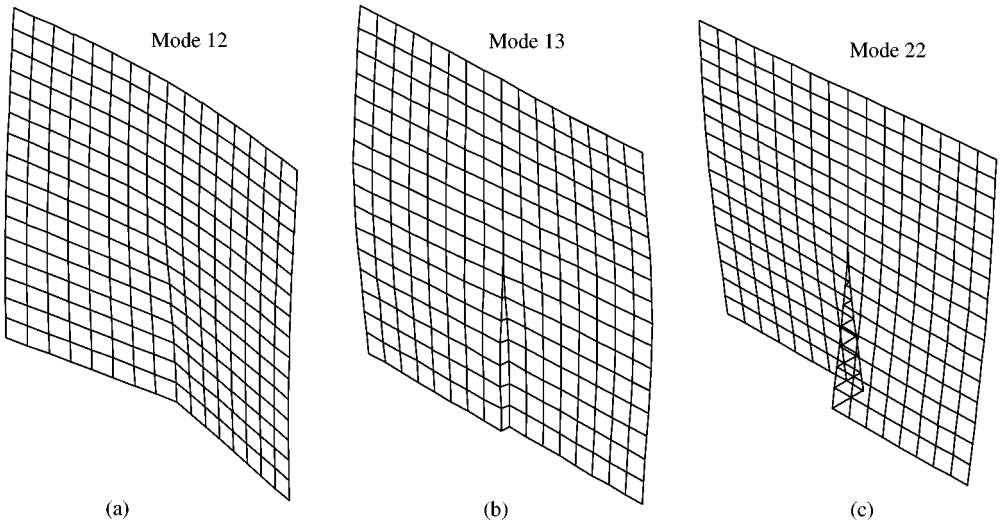

Figure 9. Natural modes of vibration of a free square plate containing a straight excavation.

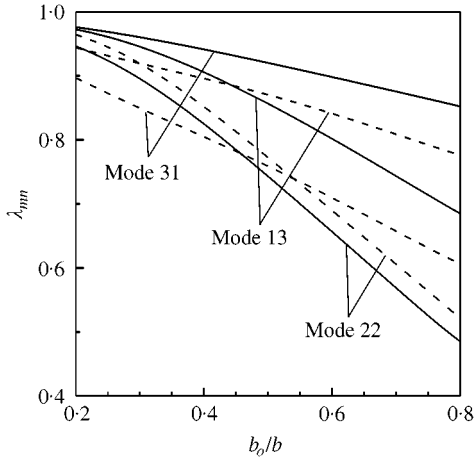

Figure 10. Influence of excavation length on natural frequencies of free plates, when $C = 2{\cdot}0$ and $\alpha_0/\alpha = 0{\cdot}50$: ——, $\alpha/b = 1{\cdot}0$; -------, $\alpha/b = 2{\cdot}0$.

half of the side, was inserted in the finite element model. Various lengths and depths of this excavation were studied and the results are discussed in the following. Figure 11 depicts the drift of some lower eigenvalues of the plate with the local flexibility coefficient C. From this figure the dependence of the eigenvalues on the arc length θ is apparent. The excavation depth interpreted by the compliance coefficient C, causes significant frequency drifts up to 40% with respect to the original ones, when full cuts are present. Figure 12 illustrates the outline of some natural modes of vibration of a free square plate with an arc-type excavation with $\theta = 45^\circ$. The discontinuities of eigenforms in this case are curved and distributed along the excavation. The effect of the excavation length interpreted by the angle θ, on the frequency drift is shown in Figure 13. A comparison with Figure 10 shows that the frequency drifts depend on excavation shapes. Thus the shape, length and depth of the laser

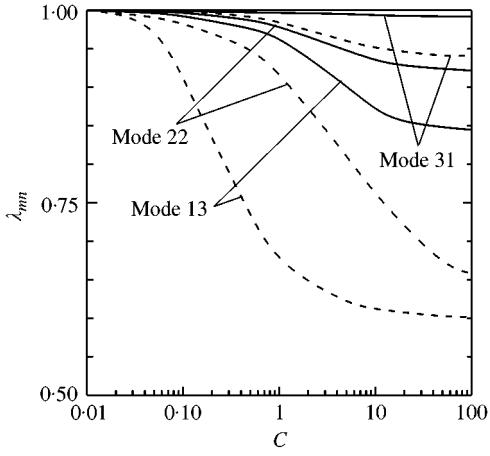

Figure 11. Drift in natural frequencies of a free square plate with a curved excavation: ——, $\theta = 30°$; ----, $\theta = 60°$.

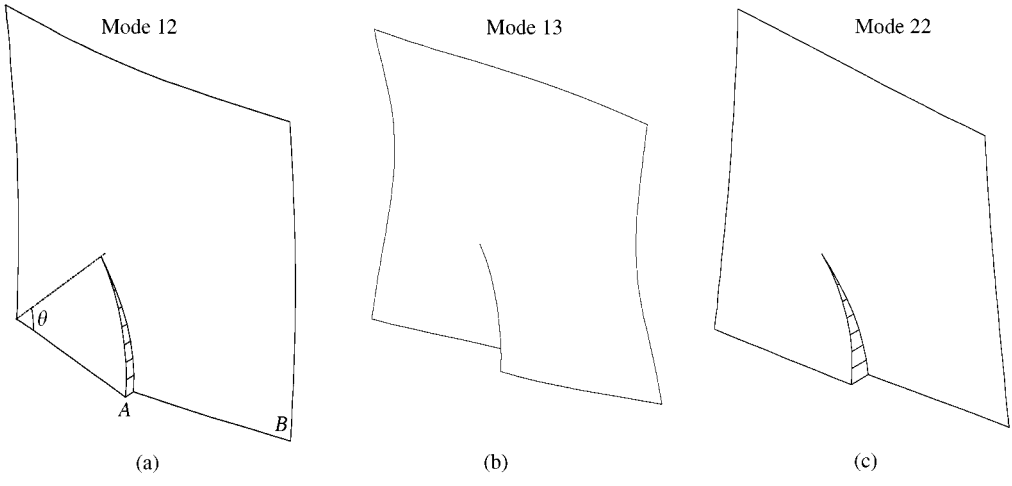

Figure 12. Eigenforms of a free square plate having a curved excavation.

process may be identified from the sequence of frequency drifts in association with discontinuities appearing in eigenforms.

The finite element formulation interpreted above is based on the framework of Mindlin plate theory and thus is limited to small deflections. However, the response is utilized during the laser process, which may induce deflections exceeding this limitation. To study this aspect, a quantitative study was conducted, in which peak values of deflection were evaluated by means of a frequency response analysis. To simulate a laser-type excitation, a concentrated transverse load was applied on the leading tip of a curved excavation (Figure 12(a)). Then, the harmonic response was numerically predicted for a free square plate, assuming the presence of light damping (5%). Figure 14 illustrates the frequency response of the points A and B which present maximum deflections. Maximum deflections occur in mode 11 and are of the order 10^{-4} m/N of applied force amplitude. As the thickness of the plate is 0·01 m and the momentum imparted by laser sources is very

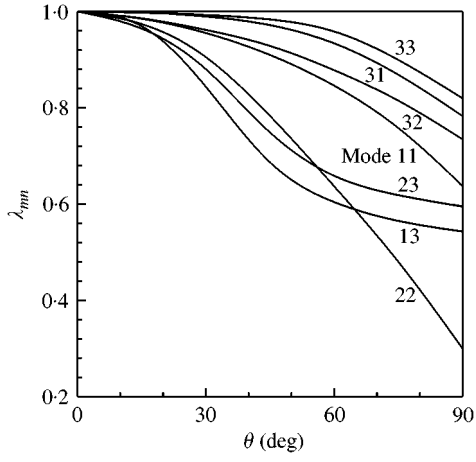

Figure 13. Influence of excavation length on the natural frequencies of a free square plate when $C = 2{\cdot}0$.

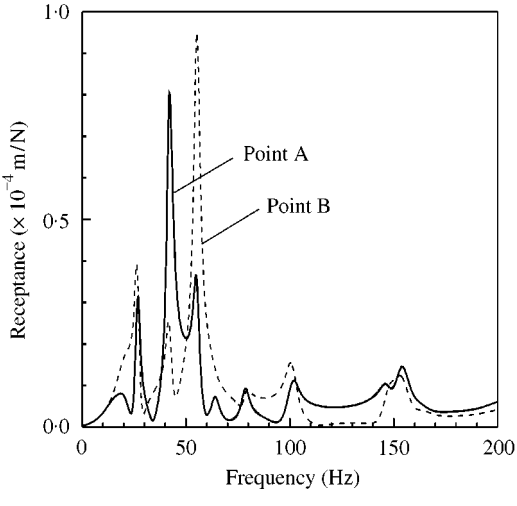

Figure 14. Harmonic response of a free square plate subjected to concentrated loading when $C = 2{\cdot}0$ and $\theta = 45^{\circ}$.

small, these results show that deflections are much less than 40% of the plate thickness as Mindlin theory assumes. Furthermore, this assumption does not restrict the applicability of the method, as alternatively thick plate elements may be utilized under finite element procedures. The eigenforms illustrated in Figures 6, 9 and 12 were normalized with respect to the mass and were drawn with the same scale factor which exaggerates deflections. Thus, the results shown in these figures may be used for comparison purposes only.

Previously reported numerical results concern two-dimensional modelling of plates incorporating line restraints of uniform strength per unit length of excavation, in an averaged sense. Three-dimensional effects arising very close to the leading tip of the excavation were neglected. The incorporation of these in the model requires application of varying discontinuity strength, especially near the leading edge of excavation. This variation yields approximately the same eigenvalues as those obtained in the uniform restraint case, and negligible changes in eigenforms near the leading edge, depending on plate thickness.

Eigenforms depend not only on the localized but mainly on the overall stiffness distribution. Thus, three-dimensional local effects change eigenforms locally and are negligible. Dynamic response seems to be much more sensitive to temperature changes because local heating causes significant material softening and thus development of very strong compliance.

With reference to previously reported numerical results, some comments may be made on the feasibility of adopting vibrational techniques to predict laser process conditioning. Considering flexible and extended workpieces, like the plate structures analyzed above, changes in the frequency response are observed which depend solely on the process characteristics. A significant frequency drop up to 50% in comparison with the initial structure, may be observed especially in the lower natural frequencies. It was proved by numerical experimentation that for each mode of vibration, the frequency shift depends directly on the length, position and depth of the laser process. When the position of the excavation is close to a vibration node, then the frequency drift is negligible as usually happens in beam structures [12]. The workpiece dimensions and supporting conditions affect significantly the frequency response. The natural modes of vibration present step discontinuities which would be utilized in a laser process conditioning method [22]. However, shallow cuts are rather difficult to be identified by the proposed method. Previous analysis gives encouraging results to adopt vibrational methods in surface laser process conditioning. Continuous monitoring of frequency response by a data acquisition system and analysis of natural modes of vibration by an image processing system may yield whole necessary information for process prediction. However, experimental verifications, more detailed investigations and sensitivity analysis are expected to give answers to most of the problems arising in the procedure application stage. This method must use finite element, image processing, data acquisition and analysis and process identification computational tools.

5. CONCLUSION

A finite element approach has been presented for the quasi-static simulation of surface laser processing procedures. This approach concerns flat rectangular plates with linear surface cuts. The subdomain method in conjunction with the distribution of spring elements along the cut to simulate the restraint introduced by the cut was utilized to approach the free vibration problem of these plates in the form of a general computational problem. From the numerical solution of this problem, imposing appropriate values to the global design variables yields information regarding the feasibility of application vibrational techniques to identify such laser processes. The numerical results obtained prove that it is possible to apply vibrational techniques for the conditioning of laser processing procedures.

REFERENCES

1. P. Di Pietro and Y. L. Yao 1994 *International Journal of Machine Tools and Manufacturing* **34**, 225–243. An investigation into characterizing and optimizing laser cutting quality—a review.
2. G. Chryssolouris 1991 *Laser Machining Theory and Practice*. New York: Springer-Verlag.
3. E. Kannatey-Asibu and D. Dornfeld 1981 *American Society of Mechanical Engineers Journal of Engineering for Industry* **107**, 330–340. Quantitative relationships for acoustic emission from orthogonal metal cutting.
4. B. A. Chin, N. H. Madsen and J. S. Goodling 1983 *Welding Journal* **38**, 227–234. Infrared thermography for sensing the arc welding process.
5. M. Y. Huang and C. R. Chatwin 1994 *Lasers in Engineering* **3**, 125–140. Spark cone characterization for control of laser cutting.

6. J. V. CANDY and D. L. LAGER 1979 Lawrence Livermore Laboratory, UCID-18270. *Identification, detection, and validation of vibrating structures: a signal processing approach.*
7. P. CAWLEY and R. D. ADAMS 1979 *Journal of Strain Analysis* **14**, 49–57. The location of defects in structures from measurements of natural frequencies.
8. M. M. KALDAS and S. M. DICKINSON 1981 *Journal of Sound and Vibration* **75**, 163–178. The flexural vibration of welded rectangular plates.
9. G. GOUNARIS, N. ANIFANTIS and A. DIMAROGONAS 1991 *Engineering Fracture Mechanics* **39**, 931–940. Dynamics of cracked hollow beams.
10. J. C. ALEXANDER and A. V. NURMIKKO 1973 *Optics Communications* **9**, 404–406. Excitation of thin elastic membranes by momentum of laser light.
11. L. L. KOSS and R. C. TOBIN 1983 *Journal of Sound and Vibration* **86**, 1–7. Laser induced structural vibration.
12. N. ANIFANTIS, R. ACTIS and A. DIMAROGONAS 1994 *Engineering Fracture Mechanics* **49**, 371–379. Vibration of cracked annular plates.
13. T. MIZUSAWA 1993 *Journal of Sound and Vibration* **163**, 193–205. Vibration of rectangular Mindlin plates by the spline strip method. doi: 10.1006/jsvi.1993.1160.
14. K. M. LIEW, K. C. HUNG and K. Y. LAM 1993 *Journal of Sound and Vibration* **163**, 451–462. On the use of the substructure method for vibration analysis of rectangular plates with discontinuous boundary conditions. doi: 10.1006/jsvi.1993.1181.
15. C. S. KIM 1995 *Journal of Sound and Vibration* **180**, 769–784. Free vibration of rectangular plates with an arbitrary straight line support. doi: 10.1006/jsvi.1995.0114.
16. I. V. ANDRIANOV and G. A. KRIZHEVSKY 1993 *Journal of Sound and Vibration* **162**, 231–241. Free vibration analysis of rectangular plates with structural inhomogeneity. doi: 10.1006/jsvi.1993.1115.
17. D. R. AVALOS, H. LARRONDO and P. A. A. LAURA 1995 *Ocean Engineering* **22**, 105–110. Transverse vibrations and buckling of circular plates of discontinuously varying thickness subject to an inplane state of hydrostatic stress.
18. H. P. LEE and T. Y. NG 1994 *Acta Mechanica* **106**, 221–230. Dynamic-response of a cracked beam subjected to a moving load.
19. H. P. LEE and T. Y. NG 1994 *Journal of Sound and Vibration* **172**, 420–427. Inplane vibration of planar frame structures. doi: 10.1006/jsvi.1994.1185.
20. L. MEIROVITCH 1967 *Analytical Methods in Vibrations*, London: The MacMillan Company.
21. P. P. LYNN and N. KUMBASSAR 1967 *Developments in Mechanics* **4**, 911–928. Free vibrations of thin rectangular plates having narrow cracks with simply supported edges.
22. A. K. PANDEY, M. BISWAS and M. M. SAMMAN 1991 *Journal of Sound and Vibration* **145**, 321–332. Damage detection from changes in curvature mode shapes.